Journal of Molecular Structure 1031 (2013) 168–174

Contents lists available at SciVerse ScienceDirect

Journal of Molecular Structure

journal homepage: www.elsevier.com/locate/molstruc

Synthesis, characterization, molecular structures, cytotoxic and antibacterial activities of *N*,*N*′-diaryl-*o*-phenylenediamines

Víctor M. Jiménez-Pérez [a,*], Marisol Ibarra-Rodríguez [a], Blanca M. Muñoz-Flores [a], Alberto Gómez [a], Rosa Santillan [b], Eugenio Hernández Fernadez [a], Sylvain Bernès [a], Noemi Waksman [c], Rosalba Ramírez Duron [c]

[a] Facultad de Ciencias Químicas, Universidad Autónoma de Nuevo León, Pedro de Alba s/n, C.P. 66451, Nuevo León, Mexico
[b] Departamento de Química, Centro de Investigación y de Estudios Avanzados del IPN, A.P. 14-740, C.P. 07000, D.F., Mexico
[c] Departamento de Química Analítica, Facultad de Medicina, PO Box 2316, Sucursal Tecnológico, 64841 Monterrey, Nuevo León, Mexico

ARTICLE INFO

Article history:
Received 4 June 2011
Received in revised form 22 August 2011
Accepted 23 August 2011
Available online 17 September 2011

Keywords:
N,*N*′-diaryl-*o*-phenylenediamine
X-ray
NMR
Biological activity

ABSTRACT

The molecular structures of *N*,*N*′-2,6-dimethylphenyl-*o*-phenylenediamine (**1**), *N*,*N*′-2,4,6-trimethylphenyl-*o*-phenylenediamine (**2**), *N*,*N*′-2,6-diisopropylphenyl-*o*-phenylenediamine **3a** and **3b** (dimorph of **3a**) have been elucidated by X-ray diffraction as well as characterized by FT-IR, HRMS, ^{1}H, ^{13}C NMR and 2D experiments. The cytotoxic and antibacterial activities of the *N*,*N*′-diaryl-*o*-phenylenediamines (**1**–**3**) were tested against human tumor cell lines A431 and MOLT4 and *Salmonella typhimurium* and *Staphylococcus aureus* respectively. Compounds **1** and **2** showed higher biological activities than compound **3** in cell line A431 and against *S. typhimurium*. Tumor cell growing was inhibited with **1** and **2** 1.0 μg/mL and 0.5 μg/mL, respectively. The minimal inhibitory concentration against *S. typhimurium* and *S. aureus* for both compounds was 0.35 μg/mL. However, all compounds presented very similar activities in cell line MOLT4 (**1**–**3**: 0.5 μg/mL) and *S. aureus* (**1**–**3:** 0.35 μg/mL). A decrease of steric hindrance on phenylenediamine derivatives might influence on biological activity.

1. Introduction

o-Phenylenediamines (*o*-PDA) derivatives have been shown as an important class of synthons in several heterocyclic [1], organic [2], organometallic [3], and coordination complexes [4]. Some phenylenediamines derivatives have been showed important biological effects such as antifungal [5], anticancer [6], and antimutagenic [7]. Also, the PDA derivatives can act as antiozonant [8], hair coloring [9], anticorrosion material [10], and nitric oxide sensor [11] (Scheme 1). The search and design of new drugs is a continuous need nowadays mainly because of the development of multiple resistance mechanisms in both bacteria and cancer cells. Besides cytotoxic activity, any chemical compound designated to be used as a new pharmacologic active substance or to improve treatment strategies, must offer possibilities in its molecular structure to be adapted in regard of enhancement of solubility, chemical stability or any other attribute focused on improving its mechanism of action.

Recently, the cytotoxicity activity against *Salmonella typhimurium* TA 102 bacteria of a short series of phenylendiamines derivatives with a structural modification on the aromatic ring has been reported. However, there is not a clear structure–activity relationship [12]. On the other hand, Hartwig and Buchwald have been developed an efficient synthetic methods to carry out a coupling reaction between 1,2-dibromoarenes and anilines [13,14]. In order to carry out a structural modification on phenylene diamines, Harlan et al. reported a simple catalyzed coupling reaction to isolated *N*,*N*-diaryl-*o*-phenylenediamine derivatives [15]. Base on that, in this paper, we describe the molecular structure and their biological activity of a short series of *N*,*N*′-aryl-*o*-phenylenediamines (Scheme 2) such as *N*,*N*′-2,6-dimethylphenyl-*o*-phenylenediamine (**1**), *N*,*N*′-2,4,6-trimethylphenyl-*o*-phenylenediamine (**2**), and *N*,*N*′-2,6-diisopropylphenyl-*o*-phenylenediamine (**3**).

2. Experimental

2.1. Reagents and measurements

All manipulations were performed under nitrogen atmosphere by using standard Schlenk techniques [16] or inside a glovebox. Toluene was dried with Na/benzophenone prior to use under N_2. Chemicals were commercial available and used as received. The compounds **1** and **3** were readily synthesized by coupling reaction of the corresponding aryl amines with 1,2-dibromobenzene [15]. Recently Hahn et al. reported the synthesis of **2** by different

* Corresponding author. Tel.: +52 8183294000; fax: +52 8183760570.
E-mail address: vjimenez@fcq.uanl.mx (V.M. Jiménez-Pérez).

0022-2860/$ - see front matter © 2012 Published by Elsevier B.V.
http://dx.doi.org/10.1016/j.molstruc.2011.08.040

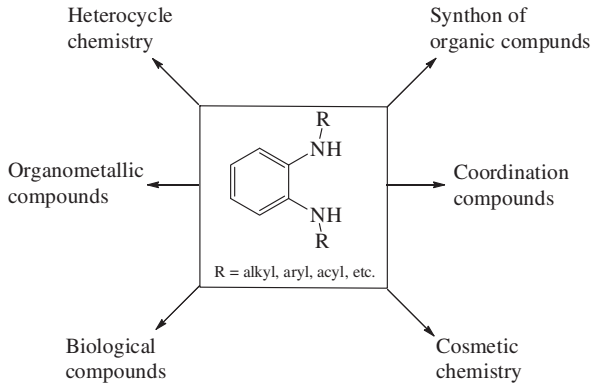

Scheme 1. *N,N′*-disubstituted-*o*-phenylenediamines derivatives on different fields.

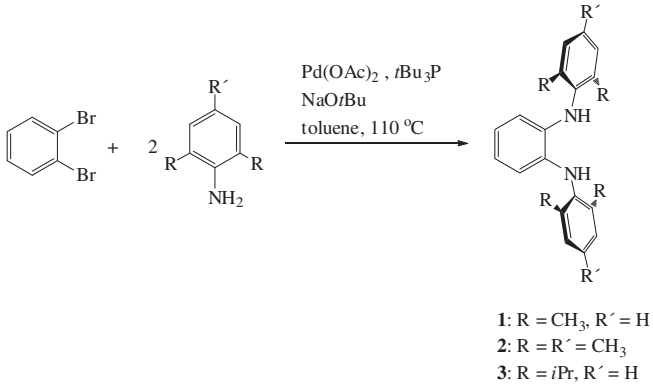

Scheme 2. Synthesis of *N,N′*-aryl-*o*-phenylenediamines **1**–**3**.

synthetic route [17]. Mass spectra in the EI mode were recorded at 20 eV on a Hewlett-Packrad HP 5989 spectrometer. High resolution mass spectra were obtained by LC/MSD TOF on an Agilent Technologies instrument with APCI as ionization source. The C_6D_6 and $CDCl_3$ were used without further purification. Melting points were obtained on a Mel-Temp II apparatus. Assignment of ^1H and ^{13}C data was performed using 2D $^1H/^{13}C$ HMBC and $^1H/^{13}C$ HSQC experiments (Supplementary data). Spectra were recorded by using Bruker 300: ^1H (300.13 MHz), ^{13}C (75.47 MHz); Bruker 400: ^1H (399.78 MHz), ^{13}C (100.52 MHz) and JEOL 400: ^1H (400.13 MHz), ^{13}C (100.61 MHz). IR spectra were obtained with FT-IR 1600 Perkin Elmer.

2.2. X-ray crystallography

Diffraction data were collected at 298 K using a Siemens P4 diffractometer equipped with the Mo Kα radiation (λ = 0.71073 Å), using standard procedure [18], and the structures refined with *SHELXL* [19]. Amine H atoms were found in difference maps and refined freely, with fixed isotropic displacement parameters. C-bonded H atoms were placed in idealized position for ordered crystals **1** and **3b**, and refined as riding to their carrier atoms. For **2**, aromatic H atoms were calculated, while methyl H atoms were refined freely with H sites splitted over two disordered equally occupied positions. Methyl geometry was however regularized with suitable soft restraints for C–H and H···H distances (see archived CIF). For **3a**, two of four isopropyl groups are disordered. Site occupation factors for disordered C atoms were refined and C–C bond lengths involved in disordered parts were restrained to 1.540(15) Å. All C-bonded H atoms were placed in idealized positions and refined as riding atoms.

2.3. In vitro cytotoxicic assay

Human epidermoid carcinoma ATCC cell line A431 and human lymphoblastic leukemia MOLT-4 were employed to test the cytotoxic effects of compounds **1**–**3**. A431 cells were maintained in Dulbecco's Modified Eagle Media (DMEM) with 4 mM L-glutamine and supplemented with 10% Foetal Bovine Serum (Gibco), 100 IU/mL penicillin and 100 μg/mL streptomycin. Culture of both cell lines was carried out at 37 °C in an Incubator (Shell Lab, TC-2323) with a 95% air and 5% CO_2 atmosphere. Leukemia cells were treated equally but cultured in RPMI culture media. Cytotoxicity of compounds **1**–**3** was tested against both cell lines at 0.5, 1.0, 5.0 and 10 ppm. Tumor cells were seeded in 24-well tissue culture plates with 5×10^4 cells/well and 24 h after platting they were supplemented by triplicate with each compound. All dilutions were prepared with fresh culture media and plates were incubated for additional 24 h. Cells in plates were washed with PBS pH = 7.4 to remove death cells. Surviving cells were measured by the MTS method [3-(4,5-dimethylthiazol-2-yl)-5-(3-carboxymethoxyphenyl)-2-(4-sulfophenyl)-2H-tetrazolium] and related to the mock cell population by measuring absorbance at 590 nm to establish cell viability with previous microscopic analysis for morphological changes exploration in cells.

2.4. Antibacterial activity

The antibacterial activity of the reported compounds was proved against *S. typhimurium* ATCC 14028 and *Staphylococcus aureus* ATCC 25923. Bacterial strains were tested in a Minimal Inhibitory Concentration assay (MIC) to determine the lowest concentration obtained by serial dilutions showing to inhibit visible growth of a microorganism after incubation. Cultures were prepared in TSB media in 96 well plates and immediately after preparation they were incubated at 37 °C during 24 h. Compounds **1**–**3** were tested against both bacterial strains from 50 ppm to 0.5 ppm. Once incubation time elapsed plates were read at 540 nm. The minimal concentration for growth inhibition was calculated by reference to each strain positive control.

2.5. Chemical synthesis of *1*–*3*

2.5.1. Synthesis of compound (*1*) *N,N′*-2,6-dimethylphenyl-o-phenylenediamine

A Schlenk flask of 500 mL was charged with $Pd(OAc)_2$ (0.22 g, 0.98 mmol) and solid tBu$_3$P (0.61 g, 3.27 mmol) in toluene (50 mL), then it was stirred until the $Pd(OAc)_2$ was dissolved. Dibromobenzene (5.9 g, 25 mmol) was added followed by 2,6-dimethyl aniline (9.1 g, 75 mmol) and NaOtBu (7.2 g, 75 mmol). The reaction mixture was heated to 110 °C for 14 h. After several hours a precipitate was formed. The flask was opened and the reaction mixture was quickly quenched with an aqueous 25 mL NH_4Cl. The toluene layer was separated and washed 2 × 80 mL water. The toluene layer was dried over $MgSO_4$ and it was flashed through silica gel (hexane/ethyl acetate (8:2)) to yield a dark green solution then concentrated until crystals began to form. The crystals were isolated by filtration and dried under vacuum; the crystals were washed with cold methanol. Yield: 7.9 g 87%. m. p. 144–146 °C. ^1H NMR (300.13 MHz, $CDCl_3$): δ = 7.18 (d, ^3J = 7 Hz, 4H, H-2 and H-4), 7.09 (t, ^3J = 7 Hz, 2H, H-3), 6.73 (dd, ^3J = 6, ^4J = 3.3 Hz, 2H, H-10), 6.36 (dd, ^3J = 6, ^4J = 3.3 Hz, 2H, H-9), 5.25 (s, 2H, H-7), 2.28 (s, 12H, H-11). ^{13}C NMR (75.45 MHz, $CDCl_3$): δ = 139.7 (C-6), 135.1 (C-8), 133.4 (C-1 and C-5), 128.8 (C-2 and C-4), 124.6 (C-3), 120.4 (C-10), 114.7 (C-9), 18.3 (C-11). HSQC correlation [δ_H/δ_C]: 2.28/18.3 [H-11/C-11], 6.36/114.7 [H-9/C-9], 6.73/120.4 [H-10/C-10], 7.09/128.8 [H-3/C-3], 7.18/133.4 [H-2, H-4/C-2, C-4]. HMBC correlation [δ_H/δ_C]: 5.25/135.1 [H-7/C-8], 6.36/120.4/135.1

[H-9/C-10/C-8], 6.73/114.7/135.1 [H-10/C-9/C-8], 7.18/133.4/139.7 [H-3/C1 and C-5/C-6], 7.18/128.8/139.7 [H-3/C2 and C-4/C-6]. MS (TOF): *m*/*z* [M+H$^+$] calcd. for $C_{22}H_{25}N_2$: 317.2012 a.m.u.; found: 317.2017 a.m.u. (error = 1.4960 ppm). MS (DIP 20 eV): *m*/*z* (%): 316 (100) [M]$^+$, 194 (20). IR (KBr) ν (cm^{-1}): 3356 (wk and shp), 3337 (wk and shp), 2941 (wk), 2911 (wk), 1587 (shp), 1471 (shp and str), 1397 (shp), 1217 (shp and str), 769 (shp and str), 747 (shp and str).

2.5.2. Synthesis of compound (**2**) N,N′-2,4,6-trimethylphenyl-o-phenylenediamine

The procedure was similar to the synthesis phenylendiamine **1**. $Pd(OAc)_2$ (0.264 g, 1.18 mmol); *t*Bu_3P (0.71 g, 3.52 mmol); 1,2-dibromo-benzene (6.9 g, 29.4 mmol); 2,4,6-trimethylaniline (7.9 g, 58.6 mmol); NaO*t*Bu (8.46 g, 87.9 mmol). The reaction mixture was heated to 110 °C for 14 h. After several hours a precipitate was formed. The flask was opened and the reaction mixture was quickly quenched with an aqueous 25 mL NH_4Cl. The toluene layer was separated and washed 2 × 80 mL water. The toluene layer was dried over $MgSO_4$ and it was flashed through silica gel (hexane/ethyl acetate (8:2)) to yield a dark green solution then concentrated until crystals began to form. The crystals were isolated by filtration and dried under vacuum; the crystals were washed with cold methanol. Yield: 7.1 g, 71%. m. p. 219 °C. ^{1}H NMR (399.78 MHz, C_6D_6): δ = 6.89 (s, 4H, H-2 and H-4), 6.70 (dd, ^3J = 5.6, ^4J = 3.6 Hz, 2H, H-10), 6.46 (dd, ^3J = 6, ^4J = 3.3 Hz, 2H, H-9), 4.78 (s, 2H, H-7), 2.25 (s, 6H, *p*-C*H*$_3$), 2.15 (s, 12H, *o*-C*H*$_3$). ^{13}C NMR (100.52 MHz, C_6D_6): δ = 137.26 (C-6), 135.43 (C-8), 134.04 (C-3), 133.76 (C-1 and C5), 129.58 (C-2 and C-4), 120.42 (C-10), 114.12 (C-9), 20.81 (*p*-*C*H$_3$), 17.96 (*o*-*C*H$_3$). MS (TOF): *m*/*z* [M+H$^+$] *calcd* for $C_{24}H_{29}N_2$: 345.500 a.m.u.; *found*: 345.2323 a.m.u. IR (KBr) ν (cm^{-1}): 3331 (wk and shp), 2914 (w), 1597 (w), 1496 (str), 1482 (str), 1398 (w), 1256 (shp), 1227 (shp), 739 (shp and str).

2.5.3. Synthesis of compound (**3**) N,N′-2,6-diisopropylphenyl-o-phenylenediamine

The procedure was similar to the synthesis phenylendiamine **1**. $Pd(OAc)_2$ (0.25 g, 1.12 mmol); *t*Bu_3P (0.68 g, 3.37 mmol); 1,2-dibromo-benzene (6.6 g, 28 mmol); 2,6-diisopropylaniline (9.90 g, 56 mmol); NaO*t*Bu (8.06 g, 84 mmol). The toluene was removed under vacuum to yield a dark solid. Methanol was added and the mixture sonicated for 30 min, to yield an off-white solid that was isolated by filtration, the solid was washed with cold methanol (2 × 10 mL) and dried under vacuum to produce an off white solid. Yield: 7.2 g, 60%. m. p. 114–116 °C. ^{1}H NMR (400.13 MHz, $CDCl_3$): δ = 7.28–7.24 (m, 6H, H-2-H-4), 6.67–6.65 (dd, ^3J = 6, ^4J = 3.6 Hz, 2H, H-10), 6.32–6.29 (dd, ^3J = 6, ^4J = 3.6 Hz, 2H, H-9), 5.24 (s, 2H, H-7), 3.25 (sept, ^3J = 7 Hz, 4H, H-11), 1.25 (d, ^3J = 7 Hz, 12H, H-12), 1.19 (d, ^3J = 7 Hz, 12H, H-13). ^{13}C NMR (100.61 MHz, $CDCl_3$): δ = 145.5 (C-8), 137.1 (C-6), 136.9 (C-1 and C5), 126.3 (C-3), 124 (C-2 and C-4), 119.5 (C-10), 114.7 (C-9), 28 (C-11), 24.0 (C-12), 23.4 (C-13). MS (TOF): *m*/*z* [M+H$^+$] *calcd.* for $C_{30}H_{41}N_2$: 429.3264 a.m.u.; *found*: 429.3261 a.m.u. (error = −0.7595 ppm). MS (DIP 20 eV): *m*/*z* (%): 428 (100) [M]$^+$, 342 (10) [M-C_6H_{14}]$^+$, 250 (25), 208 (15), 177 (7). IR (KBr) ν (cm^{-1}): 3352 (wk), 2963 (str), 2926 (wk), 2868 (wk), 1602 (wk), 1500 (wk), 1441(shp), 1263 (br and str), 741 (shp and str).

3. Results and discussion

3.1. Spectroscopic analyses

The ^{1}H NMR (at 25 °C) spectra of **1**–**3** exhibit resonances in the range from δ = 7.28 to 6.29 and 3.25 to 1.19 for aromatic and aliphatic groups respectively (Table 1). In the ^{1}H NMR spectrum of compound **3** there are three interesting features. Firstly, the H-9 protons are shifted to lower frequency than the *o*-phenylenediamine might be explained on the basis of the proximity to π-electron cloud of bulky aromatic ring. Secondly, septet of isopropyl methines (δ = 3.25 ppm) are shifted to high frequencies due to strong hydrogen bound with the lone pairs on the nitrogen atoms as is confirmed by X-ray diffraction, with a distance C–H···N 2.401(3) Å (*vide infra*). Finally, compounds **3** shown two doublets with the same intensity at δ = 1.25 (d, ^3J = 7 Hz, 12H) and 1.19 (d, ^3J = 7 Hz, 12H) of methyl groups probably due to rapid exchange of *trans* and *cis*-conformations in solution.

Assignment of ^{13}C data of compounds **1**–**3** was based on HSQC experiments (Table 2). In order to carry out an unambiguously assignment of quaternary carbon atom C-8 in compound **1**, the 2D Heteronuclear Multiple Bond Correlation (HMBC) experiment was performed. The HMBC spectrum exhibit two correlations of H-9 with C-8 and C-10. Also, the experiment indicated correlation between N–H protons (δ = 5.35 ppm) and a resonance at 135.1 ppm of C-8 (see Supplementary data).

Comparison of the IR stretching vibration of the N–H in **1**–**3** (**1:** 3356, **2:** 3331 and **3:** 3352 cm^{-1}) and the 2,6-diphenylaniline [20], clearly indicate the presence of an intramolecular hydrogen bridge towards the nitrogen atoms. The high resolution mass analyses show the molecular ions of compounds **1** [M]$^+$ 317.2012 (100), **2** [M]$^+$ 345.2323 (100), and **3** [M]$^+$ 429.3006 (100) as peak base. In both cases, the first loss observed corresponds to the bulky groups bonded to the nitrogen atom, indicating that the phenylenediamine is very stable.

Table 1
^{1}H NMR data of **1**–**3**.

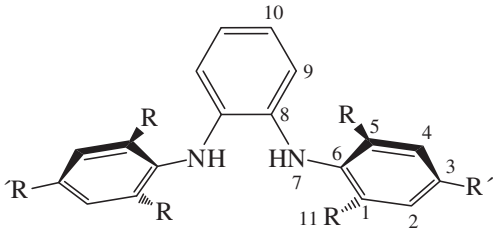

	1 ($CDCl_3$)	**2** (C_6D_6)	**3** ($CDCl_3$)
H-2 and H-4	7.18	6.89	7.27
H-3	7.09		
H-7	5.25	4.78	5.24
H-9	6.36	6.46	6.32–6.29
H-10	6.74	6.70	6.67–6.65
H-11	2.28	2.15	(*CH*(CH$_3$)$_2$) 3.25
H-12		2.25	(CH(*CH*$_3$)$_2$) 1.25, 1.19

Table 2
^{13}C NMR data of **1**–**3**.

	1 ($CDCl_3$)	**2** (C_6D_6)	**3** ($CDCl_3$)
C-1 and C-5	133.4	133.7	136.9
C-2 and C-4	128.8	129.5	124.0
C-3	124.6	134.0	126.3
C6	139.7	137.2	137.1
C-8	135.1	135.4	145.5
C-9	114.7	114.1	114.77
C-10	120.4	120.4	119.5
C-11	18.3	17.96	24.0
C-12		20.81	23.4

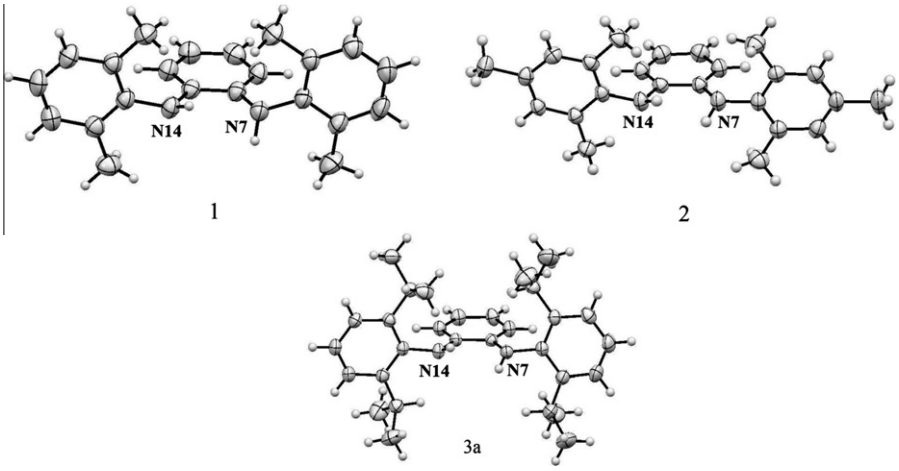

Fig. 1. Molecular structures of bulky *N*,*N*′-phenylenediamines derivatives **1**–**3**.

Table 3
Crystal data and structure refinement for compounds **1**–**3a,b**.

	1	**2**	**3a**	**3b**
CCDC	803473	803474	803475	803476
Empirical formula	$C_{22}H_{24}N_2$	$C_{24}H_{28}N_2$	$C_{30}H_{40}N_2$	$C_{30}H_{40}N_2$
Formula weight	316.43	344.48	428.64	428.64
Temperature, K	300(1)	299(1)	299(1)	300(1)
Wavelength	0.71073	0.71073	0.71073	0.71073
Cryst size, mm^3	$0.6 \times 0.4 \times 0.4$	$0.6 \times 0.2 \times 0.2$	$0.4 \times 0.4 \times 0.2$	$0.50 \times 0.30 \times 0.20$
Crystal system	Monoclinic	Triclinic	Monoclinic	Monoclinic
Space group	*P*21/*c*	*P*-1	*P*21/*c*	*P*21/*c*
Cell parameters				
a, Å	12.783(3)	8.434(7)	12.489(2)	13.512(4)
b, Å	8.888(2)	8.850(5)	12.737(4)	22.371(7)
c, Å	15.811(9)	13.972(7)	17.079(5)	8.693(3)
α	90	85.96(2)	90	90
β	96.23(4)	88.21(8)	99.34(2)	96.62(3)
γ	90	73.00(6)	90	90
V, Å^3	1785.8(12)	994.7(11)	2680.8(12)	2610.1(14)
Z, *Z*′	4,1	2, 1	4, 1	4, 1
ρ_{calc}, g cm^{-3}	1.177	1.150	1.062	1.091
μ, mm^{-1}	0.069	0.067	0.061	0.063
Data collection				
2θ range for data collection	5.18 – 50.00°	4.82 – 50.10°	4 – 50.4°	3.54 – 50.08°
Index ranges	$-15 \leqslant h \leqslant 5$, $-10 \leqslant k \leqslant 1$, $-18 \leqslant l \leqslant 18$	$-10 \leqslant h \leqslant 9$, $-10 \leqslant k \leqslant 10$, $-16 \leqslant l \leqslant 16$	$-14 \leqslant h \leqslant 9$, $-15 \leqslant k \leqslant 15$, $-20 \leqslant l \leqslant 20$	$-16 \leqslant h \leqslant 16$, $-26 \leqslant k \leqslant 1$, $-10 \leqslant l \leqslant 4$
No. of reflns collected	5260	11,199	12,743	7762
No. of indep reflns	3125	3516	4719	4604
Refinement				
[R_{int}]	6.45%	7.54%	5.89%	4.37
Goodness of fit	2.429	1.658	1.750	1.591
*R*1, w*R*2 (I > 2σ(*I*))	7.78%, 21.61%	6.02%, 15.12%	6.61%, 16.43%	5.97%, 14.69%
*R*1, w*R*2 (all data)	11.32%, 23.95%	7.50%, 16.63%	12.33%, 19.93%	10.96%, 17.49%
Largets diff peak/hole, e Å^{-3}	0.208, −0.352	0.242, −0.131	0.177, −0.192	0.179, −0.215

3.2. X-ray analysis

o-Phenylenediamines **1**, **2** and **3** are built up on a common 1,2-diaminobenzene core, with nitrogen atoms substituted by 2,6-dimethylphenyl (**1**), mesityl (**2**) or 2,6-diisopropylphenyl (**3**) groups (Fig. 1). Although they potentially display a twofold symmetry axis (C_{2v} maximum point group) and crystallize in Laue group 2/*m* or −1, in all cases the asymmetric unit contains a single molecule lying in general position. In the case of **3**, a dimorphism is observed at room temperature, in a single space group. Each form, **3a** and **3b**, has been characterized by X-ray diffraction (Tables 3–5).

The molecular conformation in the series is characterized by an arrangement of phenylamine groups nearly orthogonal to the central benzene ring, regardless of the nature of substituents in external phenyl rings. In **1**, the dihedral angles between the central benzene ring C8···C13 and phenyl groups C1···C6 and C15···C20 (see Fig 2 for numbering scheme) are 82.49(10)° and 86.44(11)°. Similar angles are found in **2**, **3a** and **3b**, in the range 78.74(7)–86.24(7)°. As a consequence, peripheral phenyl rings are expected to lie in nearly parallel planes. Compounds **1** and **2** match this feature, as reflected by dihedral angles formed by phenyl planes, 4.1(2)° and 2.06(13)°, respectively. However, some deviation is

Table 4
Selected bond distances (°) and angles (°) for **1**–**3a** and **b.**

	1	2	3a	3b
N(14)–H(14)	0.93(4)	0.88(2)	0.77(3)	0.84(3)
C(15)–N(14)	1.419(4)	1.429(2)	1.438(3)	1.431(3)
N(14)–C(13)	1.411(4)	1.403(2)	1.409(3)	1.409(3)
C(8)–N(7)	1.393(4)	1.412(2)	1.405(3)	1.402(3)
N(7)–H(7)	0.88(4)	0.92(2)	0.87(3)	0.83(3)
N(7)–C(6)	1.424(3)	1.431(2)	1.427(3)	1.433(3)
C(15)–N(14)–H(14)	112(2)	117.8(14)	116(3)	110(2)
H(14)–N(14)–C(13)	119(2)	108.9(14)	112(2)	120(2)
C(8)–N(14)–C(13)	108(2)	108.9(13)	112.9(9)	110(2)
C(13)–C(8)–N(7)	117.7(3)	118.13(14)	116.66(19)	117.56(19)
C(15)–N(14)–C(13)–C(12)	23.6(4)	−3.0(3)	15.0(4)	9.0(3)
N(14)–C(13)–C(8)–N(7)	−0.4(4)	0.5(2)	0.2(3)	−0.2(3)

Table 5
Hydrogen bonds.

	1	2	3a	3b
N7···H14	2.282	2.290	2.372	2.319
N14···H7	2.765	2.424	2.560	2.522

observed for the most bulky system, with angles as large as 13.45(13)° for form **3a** and 27.89(10)° for form **3b**. It seems that these molecules take advantage of both a degree of tetrahedral distortion for amine N atoms and restricted rotation of phenyl rings, to minimize steric hindering. Such arrangement was previously observed in related 1,2,4,5-tetrakis(amino)benzene derivatives [21], as well as in organometallics bearing *N*-heterocyclic carbene derivatives [22,23] or diimine ligands [24]. The non-parallel arrangement typical of 2,6-diisopropylphenylamine derivatives is, for example, patent in X-ray structures reported for boryllithium salts [25].

It is rather obvious that steric restrictions induced by phenyl substituents determinate the relative orientation for aromatic rings in these systems. In contrast, non-restricted diamine derivatives may adopt a non-orthogonal conformation, in order to favor intermolecular stabilizing interactions, like π···π or C–H···π contacts involving phenyl groups. An example of such a behavior has been described for 4,5-dianilinophthalamide [26], which is stabilized in the solid state with an asymmetric propeller-shaped conformation.

An important geometric feature related to the reactivity of compounds **1**–**3** is the relative orientation of lone pairs on tetrahedral N atoms. In the present study, the positions of amine H atoms H7 and H14 were determined from X-ray data, and refined freely. Despite of the limited resolution of diffraction patterns, N–H groups converged to a sensible geometry, similar along the series of studied bisamines. N–H bond lengths vary from 0.77(3) to 0.93(4) Å, and N atoms are clearly in a sp^3 hybridization state, with the largest bond angles being systematically C–N–C, *ca.* 120°, due to the steric repulsion between aromatic system substituting N atoms. Lone pairs are placed *trans* with respect to the central benzene ring, as reflected by the positions of H atoms, which point toward the α and β faces of the benzene plane (Fig. 2, inset). This arrangement, invariably found in secondary 1,2-diaminobenzene derivatives [21,22,26], avoids H···H short contacts. In **1**–**3**, amine H···H separations are however close to the sum of van der Waals radii or even shorter: the shortest H···H separation is 1.96 Å for **2** and the longest 2.34 Å for **1**. The barrier to N inversion in such diamines should be high, and N inversion is thus very unlikely to occur in solution at room temperature.

The four structures here characterized display common geometric features, and have similar conformations in the solid state. An overlay [27] carried out on non-H atoms and excluding substituents in peripheral phenyl rings shows that all the molecules indeed fit a mean conformation (Fig. 3): using geometry of **1** as a reference, root mean square deviations for fitted molecules **2**, **3a** and **3b** are 0.31, 0.17 and 0.35 Å, respectively.

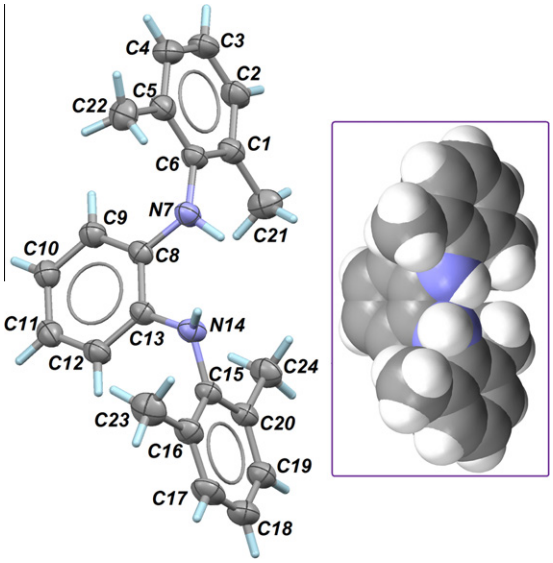

Fig. 2. *ORTEP* view of **1** with displacement ellipsoids for non-H atoms at the 25% probability level. The inset (right) is a spacefill representation of the same molecule, showing the *trans* configuration of amine NH groups.

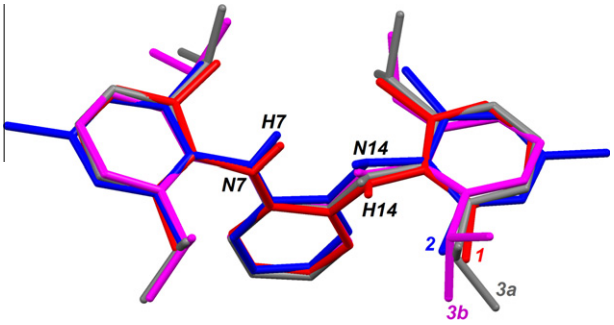

Fig. 3. Best fit between the four characterized bisamines. The overlay has been carried out using **1** as base, and by fitting aromatic C atoms and N atoms (20 atoms for each molecule) in **2**, **3a** and **3b**. C-bonded H atoms have been omitted in the figure for clarity. Color code: red: **1**, blue: **2**, gray, **3a**, magenta: **3b**. (For interpretation of the references to color in this figure legend, the reader is referred to the web version of this article.)

Table 6
Cytotoxicity assay on A431 and MOLT4 cells.

Compound	Activity[a] on A431 cells (μg/mL)	Morphological Changes in cells	Activity[a] on MOLT4 cells (μg/mL)	Morphological Changes in cells
1	1.0	Nuclei swelling and cytoplasm disturbance	0.5	Only cell debris were observed
2	0.5	Diffuse nuclei swelling and cytoplasm disturbance	0.5	Only cell debris were observed
3	5.0	Minor cytoplasm disturbances	0.5	Only cell debris were observed

[a] Minimal concentration showing toxic effects on both cell lines.

Table 7
Minimal inhibitory concentration for bacteria.

Compound	Bacterial strain ATCC (μg/mL)	
	Salmonella typhimurium 14028	*Staphylococus aureus* 25923
1	0.35	0.35
2	0.35	0.35
3	0.75	0.35

Finally, this geometry dictated mainly by steric factors, is unfavorable for efficient packing in the crystals. Instead, molecules are well separated, and no significant intermolecular interactions are available for crystal stabilization. The packing index [28] computed for **1**, **2** and **3b** (non-disordered crystals) is consistent with poorly packed molecules: 0.669 (**1**), 0.699 (**2**) and 0.646 (**3b**). This characteristic also explains why these compounds afford poorly diffracting samples, and why methyl groups have disordered H atoms positions, due to a degree of free rotation about their C–C bonds. In the present case, this disorder has been modeled for all methyl groups in **2**, although it is also probably present in **1** and **3**. The dimorphism observed in **3** may also be rationalized on the basis of non-flexible, poorly packed molecules. Dynamic motions for isopropyl substituents allow to stabilize [29] disordered (**3a**) and non-disordered (**3b**) concomitant crystals, which display different crystal structures.

3.3. Biological activity

The *in vitro* cytotoxic assay showed that compounds **1**–**3** have a toxic effect against A431 cancer cells and MOLT4 leukemic cells. The resume of cytotoxic activities of all compounds is given in Table 6. On A431 cells, compound **1** started to be active at 1.0 μg/mL. Some morphological changes and nuclei swelling and cytoplasm disturbance were observed. Similar results were found with compound **2** where a more diffuse nuclei swelling and cytoplasm disturbances were evident and clear. It appears to be more active starting to be cytotoxic at 0.5 μg/mL. In contrast, cytotoxic activity of compound **3** is lower compared to the former two compounds (5.0 μg/mL) regardless of the slight effects on cell morphology. Similar results were obtained for the three compounds when tested on MOLT4 cells, but in this cell line each compound showed activity at 0.5 μg/mL.

The synthesized compounds where screened by a turbidimetric method and all of them showed antibacterial activity. The corresponding MIC values for compounds **1** and **2** against *S. typhimurium* and *S. aureus* were established at 0.35 μg/mL. Compound **3** also presented activity against both bacterial strains but with different MIC values. For *S. typhimurium* the growth inhibition was reached at 0.75 μg/mL meanwhile *S. aureus* was inhibited at 0.35 μg/mL (Table 7). Based on these cytotoxic and antibacterial results, it seems that the steric effect of *N*-aryl groups on *o*-phenylendiamines is a significant factor in cell line A431 and against *S. typhimurium*. However, all compounds presented very similar activities in cell line MOLT4 (**1**–**3**: 0.5 μg/mL) and *S. aureus* (**1**–**3:** 0.5 μg/mL).

4. Conclusions

In summary, we report the characterization and molecular structures of three *N*,*N*′-diaryl-*o*-phenylenediamine derivatives. In all cases the arrangement of phenylamine groups nearly orthogonal to the central benzene ring. In the case of the more sterically demanding phenylenediamine (**3**) showed dimorphism. A decrease of steric hindrance on *o*-phenylendiamines might influence on biological activity.

Acknowledgements

This work was supported by CONACYT (Grant: 82605) and PAICYT-UANL (IT-160-09). M. I.-R. thanks for scholarship from CONACYT.

Appendix A. Supplementary material

High resolution mass spectrometry and spectroscopic data for compounds **1**–**3**. X-ray crystallographic data in the CIF format of the reported structures has been deposited with the Cambridge Crystallographic Data Centre. CCDC reference numbers 803473(**1**), 803474(**2**), 803475(**3a**) and 803476(**3b**). Copies of the data can be obtained free of charge on application to CCDC, 12 Union Road, Cambridge CB21EZ, UK (fax: +44 1223 336 033; e-mail: deposit@ccdc.cam.ac.uk). Supplementary data associated with this article can be found, in the online version, at doi:10.1016/j.molstruc.2011.08.040.

References

[1] C.N. Raut, S.M. Bagul, R.A. Janrao, S.D. Vaidya, V.B.S. Kumar, P.P. Mahulikar, J. Heterocycl. Chem. 47 (2010) 582.
[2] X.H. Zeng, M. Liu, M.W. Ding, H.W. He, Synth. Commun. 40 (2010) 1453.
[3] A.V. Zabula, F.E. Hahn, Eur. J. Inorg. Chem. (2008) 5165.
[4] Y. -B Huang, G.-R. Tang, G.-Y. Jin, G.-X. Jin, Organometallics 27 (2008) 259.
[5] G.J. Niemann, J. Dekker, Neth. J. Plant Pathol. 72 (1966) 213.
[6] I. Bouabdallah, L.A. ḾBarek, A. Zyad, A. Ramdani, I. Zidane, A. Melhaoui, Nat. Prod. Res. 20 (2006) 1024.
[7] E.E. Obaseiki-Ebor, K. Odukoya, H. Telikepalli, L.A. Mitscher, D.M. Shankel, Mutat. Res. 302 (1993) 109.
[8] R.H. Krüger, C. Boissiére, K. Klein-Hartwig, H.J. Kretzschmar, Food Addit. Contam. 22 (2005) 968.
[9] [a] I.J. Kang, M.H. Lee, Contact Dermatitis 55 (2006) 26;
[b] F. Hueber-Becker, G.J. Nohynek, W.J. Meuling, F. Benech-Kieffer, H. Toutain, Food Chem. Toxicol. 42 (2004) 1227.
[10] H.P. Sachin, M.H. Moinuddin Khan, N.S. Bhujangaiah, Int. J. Electrochem. Sci. 4 (2009) 134.
[11] M.N. Friedemann, S.W. Robinson, G.A. Gerhardt, Anal. Chem. 68 (1996) 2621.
[12] H. Yu, M. Foreman, J. Choi, S. Wang, Food Chem. Toxicol. 46 (2008) 3780.
[13] J.F. Hartwig, Angew. Chem. Int. Ed. 37 (1998) 2046.
[14] J.P. Wolfe, S. Wagaw, J.-F. Marcoux, S.L. Buchwald, Acc. Chem. Res. 31 (1998) 805.
[15] T. Wenderski, K.M. Light, D. Ogrin, S.G. Bott, C.J. Harlan, Tetrahedron Lett. 45 (2004) 6851.
[16] D.F. Shriver, M.A. Drezdon, The Manipulation of Air-Sensitive Compounds, 2nd ed., Wiley, New York, 1986.
[17] J.V. Dickschat, S. Urban, T. Pape, F. Glorius, F.E. Hahn, Dalton Trans. 39 (2010) 11519.
[18] XSCANS (Version 2.31). Siemens Analytical X-ray Instruments Inc., Madison, Wisconsin, USA, 1996.
[19] G.M. Sheldrick, Acta Cryst. A 64 (2008) 112.

[20] M. Tanabiki, K. Tsuchiya, Y. Kumanomido, K. Matsubara, Y. Motoyama, H. Nagashima, Organometallics 23 (2004) 3976.
[21] D.M. Khramov, A.J. Boydston, C.W. Bielawski, Org. Lett. 8 (2006) 1831.
[22] H. Sakurai, K. Sugitani, T. Moriuchi, T. Hirao, J. Organomet. Chem. 690 (2005) 1750.
[23] S. Urban, M. Tursky, R. Fröhlich, F. Glorius, Dalton Trans. (2009) 6934.
[24] Y.B. Huang, G.R. Tang, G.Y. Jin, G.X. Jin, Organometallics 27 (2008) 259.
[25] Y. Segawa, Y. Suzuki, M. Yamashita, K. Nozaki, J. Am. Chem. Soc. 130 (2008) 16069.
[26] U. Trinks, E. Buchdunger, P. Furet, W. Kump, H. Mett, T. Meyer, M. Müller, U. Regenass, G. Rihs, N. Lydon, P. Traxler, J. Med. Chem. 37 (1994) 1015.
[27] C.F. Macrae, I.J. Bruno, A.J. Chisholm, P.R. Edgington, P. McCabe, E. Pidcock, L. Rodríguez-Monge, R. Taylor, J. van de Streek, P.A. Wood, J. Appl. Cryst. 41 (2008) 466.
[28] A.L. Spek, J. Appl. Cryst. 36 (2003) 7.
[29] S.L. Price, Acc. Chem. Res. 42 (2009) 117.